Mid-infrared reflectivity of experimental atheromas

Hoi-Ying N. Holman,[a,*] Kathy A. Bjornstad,[a] Michael C. Martin,[a] Wayne R. Mckinney,[a] Eleanor A. Blakely,[a] and Francis G. Blankenberg[b]
[a]University of California, Berkeley, Lawrence Berkeley National Laboratory, Berkeley, California 94720
[b]Stanford University, Stanford, California 94305

Abstract. We report that the pathologic components present within the atheromatous plaques of ApoE knockout mice can reflect significant amounts of mid-infrared (mid-IR) light. Furthermore, the reflected light spectra contained the unique signatures of a variety of biologic features including those found in unstable or "vulnerable" plaque. This discovery may represent a unique opportunity to develop a new intravascular diagnostic modality that can detect and characterize sites of atherosclerosis.

[DOI: 10.1117/1.2937469]

Keywords: spectroscopy; reflectance; optical character recognition; optical properties; molecular spectroscopy; infrared imaging.

Paper 08030LR received Jan. 24, 2008; revised manuscript received Mar. 20, 2008; accepted for publication Mar. 26, 2008; published online Jun. 27, 2008.

Vulnerable plaques (VPs) are metabolically active and histologically complex atheromas that are prone to spontaneous rupture often leading to sudden death.[1] Coronary angiography cannot distinguish between a VP and a stable plaque. Mid-infrared (mid-IR) spectroscopy has been used previously to characterize the biochemical changes within thin sections of atheromas including VPs *ex vivo*.[2–5] A variety of absorption peaks and bands within the mid-IR transmission spectra have been specifically linked to the vibrations of atoms within atherogenic lipoproteins, phospholipid particles, cholesterol esters, and fatty acids. Unfortunately, the high native water content within the arterial wall and its strong interfering absorption has severely limited the use of mid-IR spectroscopy. Alternative methods can circumvent these difficulties, including spectral analyses of the absorption patterns from "reflected" as opposed to "transmitted" infrared light, coupled to a bright but harmless light emitter such as a synchrotron.[6] In this article, we describe how mid-IR light is reflected by pathologic components in the diseased aortic intima of ApoE(-/-) mice. The reflected light also contains the spectral signatures of the pathologic molecules within atheromas including VPs.

Reflection-based mid-IR spectroscopy is a well-established technique, and due to its unique contrast mechanism, it has been widely used for the characterization and structure-property elucidation of multilayered materials.[7] We have previously extended this technique to measure the reflection-absorption Fourier transform infrared spectra (FTIR) of microbial communities located on geological materials that contain multiple reflective interfaces of different optical properties.[6] We postulated that this technique could also be applied to whole tissues in which a subsurface change in refractive index creates a reflective interface among the pathologic molecules of interest. This type of interface exists within the intima of atherosclerotic vessels where non-native lipid (average refractive indicies of 1.45 to 1.50, depending on composition and sizes of lipid particles[8]) and calcium deposits like hydroxylapatite or calcium phosphate (average refractive index of at least 1.63[9]) are found in great abundance. Normal intimal tissues are ~80% water content, relatively uniform in optical properties, and have an average refractive index of approximately 1.35 to 1.38 (by extrapolation from the literature).[10,11] Although these refractive indices are for visible light, they may approximate the differences within the complex atherosclerotic matrix.

Conceptually, mid-IR light that enters an atheroma should encounter multiple refractive boundaries, wherein some light might be reflected and reemerge. From first principles, if the surface roughness at the refractive boundary is larger than the wavelength of the incoming light, the light that is not absorbed would undergo multiple diffuse reflections before reemerging. If the surface roughness is smaller than the wavelength (nearly smooth), unabsorbed light can experience a quasi-specular reflection before reemerging. The lack of information about the wavelength-dependent refractive index, absorption coefficients, and the surface roughness of atherosclerotic interfaces makes it difficult to predict reflectivity. Given the morphologic complexity of most atheromas, the final signal would likely be the sum of these two modes of reflectivity. It is also likely that the features of the reflected infrared spectra would contain the absorption patterns generated by the major pathologic components of an atheroma, namely, atherogenic lipoproteins, extracellular phospholipid particles, smooth muscle cells, foam cells, and disintegrating foam cells as they undergo apoptotic cell death.[12]

We made infrared measurements on the explanted aorta of a 9-month-old female adult ApoE(-/-) mouse. ApoE(-/-) (*Apoe*^{tm1Unc}) and wild-type mice were obtained from Jackson Laboratories (Bar Harbor, Maine). ApoE(-/-) mice were placed on a high fat/cholesterol (1 to 2%) diet for 3 months

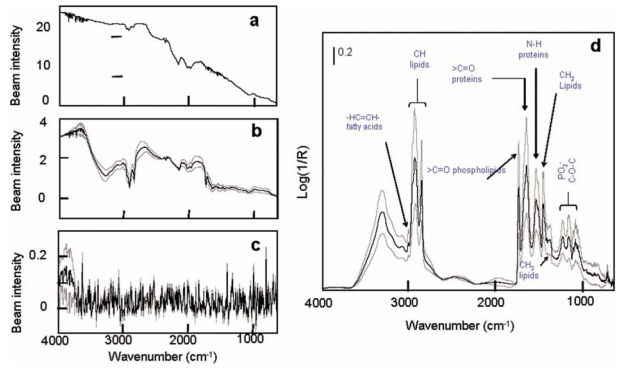

Fig. 1 Typical intensity profiles of (a) the incoming synchrotron infrared beam, (b) reflected signals from atheromas, and (c) nonatherosclerotic sites. (d) The corresponding reflection-absorption spectra of (b) shared spectral characteristics that were consistent with known excitation effects by infrared photons on atoms of molecules that compose atheromas. Each plot shows the averaged spectrum (black line) ±1.0 standard deviation (gray line); $n=26$.

*Tel: 650–497–8601; 510–486–5943; E-mail: blankenb@stanford.edu; hyholman@lbl.gov

until sacrifice. We employed Beamline 1.4.3 at the advanced light source (ALS) synchrotron at LBNL (http://infrared.als.lbl.gov/). The synchrotron infrared beam has brightness of approximately 10^{11} to 7×10^{12} photons/s-mm^2 mrad-0.1%BW when focused to a 10-μm spot. Specimens were placed luminal side up beneath an infrared-transparent ZnSe window (International Crystal Labs, New Jersy) inside a custom-built environmental chamber kept at ~5 °C to preserve the "freshness" of each specimen. FTIR measurements were recorded in the standard reflection mode in the mid-IR 4,000 to 650 cm^{-1} region, and consisted of 128 co-added spectra at a spectral resolution of 4 cm^{-1}. We found that a highly focused beam (10 to 20 μm) was needed to avoid the interference of water from nondiseased regions and that a focal spot of 150 μm or greater could not resolve plaque spectra separate from water signal. We also found that FTIR measurements could be obtained even through a 10-μm layer of water.

Figure 1 shows examples of the FTIR measurements from a cluster of atheromas including VPs (confirmed later by histologic examination) within the aortic arch. A significant number of mid-IR photons [Fig. 1(a)] that entered any given atheroma were reflected and emerged from the tissue sample [Fig. 1(b)]. In contrast, few were reflected from the nondiseased portions of aorta [Fig. 1(c)]. A striking feature was that the reflected light contained the spectral features [Fig. 1(d)] associated with atheromas.[3–5] For instance, the 3100 to 2800 cm^{-1} region revealed similar spectral features that arise from the carbon hydrogen bond stretching vibrations of fatty acids and cholesterol esters, including the –HC=CH– moiety of their unsaturated hydrocarbon chains at ~3010 cm^{-1} or from their acyl CH_2 groups at ~2925 and ~2852 cm^{-1}. The strong absorption at ~1745 cm^{-1} also matched the spectral profile of the C=O stretching vibrations of ester carbonyl (>C=O) groups of atherogenic phospholipid. The broader absorptions in the 1700 to 1500 cm^{-1} region had comparable features to those generated by the >C=O stretching of the amide I and of the N–H bending of the amide II modes present in proteins. In the 1500 to 1000 cm^{-1} fingerprint region, absorption characteristics at ~1465 and ~1375 cm^{-1} were similar to the known vibrations of the lipid acyl CH_2 and to the symmetric bending of the lipid methyl CH_3 groups, respectively. The absorptions at ~1240 and ~1090 cm^{-1} matched the spectral patterns that arise from the asymmetric and symmetric stretching modes of PO_2^- in the phosphodiester groups of phospholipids, whereas absorptions centered at ~1165 cm^{-1} and ~1060 cm^{-1} matched the ester C–O–C vibrations of phospholipid, cholesterol ester and fatty acid.[3–5]

A dendrographic analysis of all FTIR measurements (employing d-value distances measure, Ward's algorithm, together with the distribution of the z values, not shown) suggested that our spectra data could be grouped into four categories (I to IV) [Figs. 2(a)–2(d); black lines], based on their similarity. To determine whether the observed spectral patterns of reflected light could be linked to particular patho-

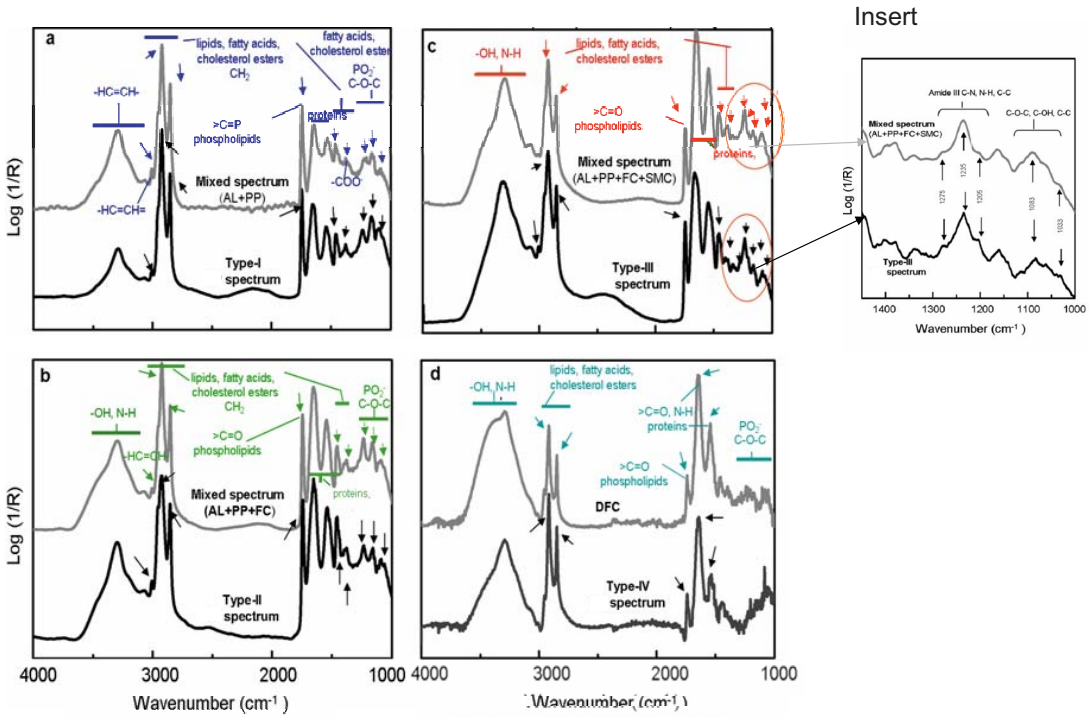

Fig. 2 (a) Spectral variations in the type-I spectrum of atheromas (black line) can be explained (see text) by the two-component model spectrum of mixed AL+PP (gray line). (b) Spectral variations in the type-II spectrum of atheromas (black line) can be explained (see text) by the three-component model spectrum of mixed AL+PP+FC (gray line). (c) Spectral variations in the type-III spectrum of atheromas (black line) can be explained (see text) by the four-component model spectrum of AL+PP+FC+SMC (gray line). Inset: a close-up comparison of the type-III spectrum of atheromas (black line) with the composite spectrum of AL+PP+FC+SMC (gray line). The triplet of peaks in 1300 to 1200 cm^{-1} and the doublet of peaks in 1100 to 1000 cm^{-1} closely match the typical spectral pattern of type-I collagen (see text). (d) Spectral variations in the type-IV spectrum of atheromas (black line) can be explained (see text) by the spectrum of DFC (gray line). R, reflectance; AL, atherogenic lipoproteins; PP, phospholipid particles; AM, activated macrophages; FC, late-stage foam cells; DFC disintegrating foam cells, and SMC, smooth muscle cells.

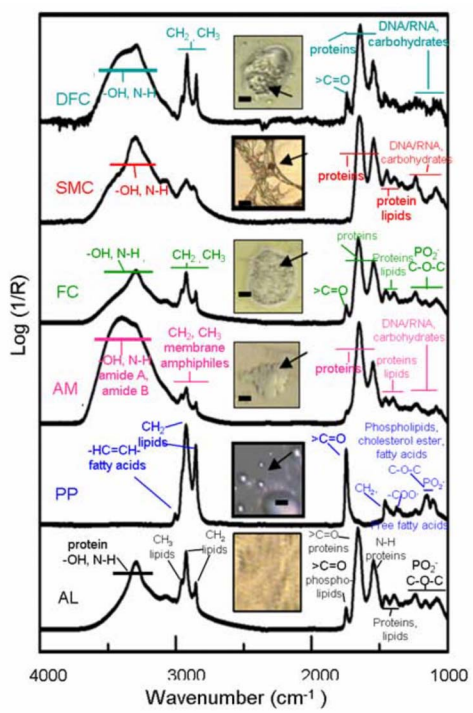

Fig. 3 Photomicrographs and reflection-absorption FTIR spectra of AL, PP, AM, FC, SMC, and DFC are displayed. Each spectrum is an average of at least 20 different samples. Purified chicken egg yolk and lipopolysaccharides from *Salmonella minnesota* were purchased from Sigma-Aldrich (Missouri). J744A.1 murine macrophage cells were obtained from the American Tissue Culture Collection (ATCC). Thin films of egg yolk[14] were prepared from the powder of the purified egg yolk, which was suspended in distilled sterile water and dried under a stream of nitrogen gas. We recorded the spectra of extracellular PL and SMC that were isolated from transverse microdissections of frozen ApoE(-/-) mouse tissues. To obtain spectra of macrophage and macrophage-derived foam cells, we activated mouse macrophages (J744A.1) in culture with bacterial molecules and obtained foam cells by feeding the activated macrophages cholesterol-containing liposomes. The spectra of each stage of foam cell evolution were measured at 24 h (early-stage cells), 48 h (mature), and 72 h (late). For DFCs, we fed activated macrophages excess cholesterol-containing liposomes for 96 h. Scale bars PP, 5 μm; AM, FC, and DFC, 10 μm; and SMC, 15 μm.

logic features, we conducted additional FTIR measurements on several model systems, (Fig. 3) & [Figs. 2(a)–2(d); gray lines].

We found that the type-I spectrum [Fig. 2(a), black lines], based on its spectral shape and the sharply defined high absorptions (at ~2925, ~2852, ~1745, ~1465, ~1375, ~1240, ~1165, ~1090, and ~1060 cm^{-1}), indicates the dominant presence of lipoproteins and phospholipids [Fig. 3(a); gray line]. For the type-II spectrum [Fig. 2(b); black line], its overall spectral shape indicates the presence of foam cells [Fig. 2(b); gray line] in addition to lipoprotein and phospholipid; a characteristic of VPs. The type-III spectrum exhibits a fine structure of a triplet of peaks at ~1275, ~1235, and ~1205 cm^{-1}, and a doublet of peaks at ~1083 and ~1033 cm^{-1} [Fig. 2(c); black line], are indicative of type-I collagen[3,5] and possibly smooth muscle cells [Fig.2(c); gray line]. Smooth muscle cells in VPs that have been reported to orchestrate the assembly of type-I collagen.[13] Finally, the type-IV spectrum [Fig. 2(d); black line] exhibits spectral features in the region >1400 cm^{-1} typical of the disintegrating foam cells [Fig. 2(d); gray line], especially the spectral region between 1200 and 1000 cm^{-1}, in which there was a conspicuous absence of the PO_2^- group absorption peaks that are characteristic of nucleic acids and various oligo- and polysaccharides, most of which were probably degraded during apoptotic cell death.

We then repeated FTIR measurements on the diseased aortas from another three ApoE(-/-) mice (3-month-old adult females) and two wild-type controls and found similar results. Further studies are required to determine whether these new findings can be translated to the diseased vessels of other animal models or humans.

Acknowledgments

US Department of Energy: 76SF00098, 05CH11231.

References

1. M. Gossl, et al., "Vulnerable plaque: detection and management," *Med. Clin. North Am.* **91**(4), 573–601 (2007).
2. J. M. Gentner, E. Wentrup-Byrne, P. J. Walker, and M. D. Walsh, "Comparison of fresh and post-mortem human arterial tissue: an analysis using FT-IR microspectroscopy and chemometrics," *Cell. Mol. Biol. (Paris)* **44**(1), 251–259 (1998).
3. K. Z. Liu, I. M. C. Dixon, and H. H. Mantsch, "Distribution of collagen deposition in cardiomyopathic hamster hearts determined by infrared microscopy," *Cardiovasc. Pathol.* **8**(1), 41–47 (1999).
4. A. Becker, M. Epple, K. M. Muller, and I. Schmitz, "A comparative study of clinically well-characterized human atherosclerotic plaques with histological, chemical, and ultrastructural methods," *J. Inorg. Biochem.* **98**(12), 2032–2038 (2004).
5. D. L. Wetzel, G. R. Post, and R. A. Lodder, "Synchrotron infrared micro spectroscopic analysis of collagens I, III, and elastin on the shoulders of human thin-cap fibroatheromas," *Vib. Spectrosc.* **38**(1–2), 53–59 (2005).
6. H.-Y. N. Holman and M. C. Martin, "Synchrotron radiation infrared spectromicroscopy: a non-invasive molecular probe for biogeochemical processes," in *Advances in Agronomy*, D. Sparks, Ed., pp. 79–127, Elsevier, New York (2006).
7. M. Claybourn, "Mid-infrared external reflection spectroscopy," in *Handbook of Vibrational Spectroscopy*, J. M. Chalmers and P. R. Griffiths, Eds., pp. 969–981, Wiley Interscience, London (2002).
8. V. P. Maltsev, A. V. Chernyshev, K. A. Semyanov, and E. Soini, "Absolute real-time determination of size and refractive index of individual microspheres," *Meas. Sci. Technol.* **8**(9), 1023–1027 (1997).
9. B. J. Tarasevich, C. C. Chusuei, and D. L. Allara, "Nucleation and growth of calcium phosphate from physiological solutions onto self-assembled templates by a solution-formed nucleus mechanism," *J. Phys. Chem. B* **107**(38), 10367–10377 (2003).
10. L. J. J. Dirckx, L. C. Kuypers, and W. F. Decraemer, "Refractive index of tissue measured with confocal microscopy," *J. Biomed. Opt.* **10**(4), 044014 (2005).
11. H. D. Downing and D. Williams, "Optical-constants of water in infrared," *J. Geophys. Res.* **80**(12), 1656–1661 (1975).
12. P. Libby and P. Theroux, "Pathophysiology of coronary artery disease," *Circulation* **111**(25), 3481–3488 (2005).
13. M. M. Kockx, et al., "Cell composition, replication, and apoptosis inatherosclerotic plaques after 6 months of cholesterol withdrawal," *Circ. Res.* **83**(4), 378–387 (1998).
14. D. Kritchevsky, "Dietary-protein, cholesterol and atherosclerosis—a review of the early history," *J. Nutr.* **125**(3), S589–S593 (1995).